



Calhoun: The NPS Institutional Archive
DSpace Repository

Theses and Dissertations

1. Thesis and Dissertation Collection, all items

2020-12

CARBON NANOTUBE REINFORCEMENT IN COMPOSITE CYLINDERS

Shelley, Dustin A.

Monterey, CA; Naval Postgraduate School

<http://hdl.handle.net/10945/66719>

this publication is a work of the U.S. Government as defined in Title 17, United States Code, Section 101. Copyright protection is not available for this work in the United States.

Downloaded from NPS Archive: Calhoun



<http://www.nps.edu/library>

Calhoun is the Naval Postgraduate School's public access digital repository for research materials and institutional publications created by the NPS community. Calhoun is named for Professor of Mathematics Guy K. Calhoun, NPS's first appointed -- and published -- scholarly author.

Dudley Knox Library / Naval Postgraduate School
411 Dyer Road / 1 University Circle
Monterey, California USA 93943



NAVAL POSTGRADUATE SCHOOL

MONTEREY, CALIFORNIA

THESIS

CARBON NANOTUBE REINFORCEMENT IN COMPOSITE CYLINDERS

by

Dustin A. Shelley

December 2020

Thesis Advisor:

Young W. Kwon

Co-Advisor:

John Molitoris,

Lawrence Livermore National Laboratory

Approved for public release. Distribution is unlimited.

THIS PAGE INTENTIONALLY LEFT BLANK

REPORT DOCUMENTATION PAGE			<i>Form Approved OMB No. 0704-0188</i>	
Public reporting burden for this collection of information is estimated to average 1 hour per response, including the time for reviewing instruction, searching existing data sources, gathering and maintaining the data needed, and completing and reviewing the collection of information. Send comments regarding this burden estimate or any other aspect of this collection of information, including suggestions for reducing this burden, to Washington headquarters Services, Directorate for Information Operations and Reports, 1215 Jefferson Davis Highway, Suite 1204, Arlington, VA 22202-4302, and to the Office of Management and Budget, Paperwork Reduction Project (0704-0188) Washington, DC, 20503.				
1. AGENCY USE ONLY (Leave blank)		2. REPORT DATE December 2020		3. REPORT TYPE AND DATES COVERED Master's thesis
4. TITLE AND SUBTITLE CARBON NANOTUBE REINFORCEMENT IN COMPOSITE CYLINDERS				5. FUNDING NUMBERS
6. AUTHOR(S) Dustin A. Shelley				
7. PERFORMING ORGANIZATION NAME(S) AND ADDRESS(ES) Naval Postgraduate School Monterey, CA 93943-5000				8. PERFORMING ORGANIZATION REPORT NUMBER
9. SPONSORING / MONITORING AGENCY NAME(S) AND ADDRESS(ES) N/A				10. SPONSORING / MONITORING AGENCY REPORT NUMBER
11. SUPPLEMENTARY NOTES The views expressed in this thesis are those of the author and do not reflect the official policy or position of the Department of Defense or the U.S. Government.				
12a. DISTRIBUTION / AVAILABILITY STATEMENT Approved for public release. Distribution is unlimited.				12b. DISTRIBUTION CODE A
13. ABSTRACT (maximum 200 words) High specific strength and stiffness properties of carbon fiber composite cylinders make them an ideal material for internal pressure and blast applications. While previous research investigates failure loading and modes on composite cylinders, additional studies display the benefits of carbon nanotube (CNT) reinforcement in various applications. However, limited research has been conducted on the effects of CNT reinforcement with respect to internal pressure loading. CNT reinforcement in composite cylinders could result in significant improvements in specific strength and stiffness, allowing for higher internal pressure loading. In this work, using wet winding, CNTs were distributed into resin and then introduced into a fiber matrix. Composite cylinders were produced at various winding angles. These cylinders were tested and compared to cylinders without CNT reinforcement. This research focuses on the specific strength and stiffness of CNT-reinforced cylinders.				
14. SUBJECT TERMS carbon nanotube, CNT, composite, CNT reinforcement, nano, nanomaterial, specific strength				15. NUMBER OF PAGES 73
				16. PRICE CODE
17. SECURITY CLASSIFICATION OF REPORT Unclassified		18. SECURITY CLASSIFICATION OF THIS PAGE Unclassified		19. SECURITY CLASSIFICATION OF ABSTRACT Unclassified
				20. LIMITATION OF ABSTRACT UU

THIS PAGE INTENTIONALLY LEFT BLANK

Approved for public release. Distribution is unlimited.

CARBON NANOTUBE REINFORCEMENT IN COMPOSITE CYLINDERS

Dustin A. Shelley
Lieutenant, United States Navy
BS, Virginia Military Institute, 2013

Submitted in partial fulfillment of the
requirements for the degree of

MASTER OF SCIENCE IN MECHANICAL ENGINEERING

from the

**NAVAL POSTGRADUATE SCHOOL
December 2020**

Approved by: Young W. Kwon
Advisor

John Molitoris
Co-Advisor

Garth V. Hobson
Chair, Department of Mechanical and Aerospace Engineering

THIS PAGE INTENTIONALLY LEFT BLANK

ABSTRACT

High specific strength and stiffness properties of carbon fiber composite cylinders make them an ideal material for internal pressure and blast applications. While previous research investigates failure loading and modes on composite cylinders, additional studies display the benefits of carbon nanotube (CNT) reinforcement in various applications. However, limited research has been conducted on the effects of CNT reinforcement with respect to internal pressure loading. CNT reinforcement in composite cylinders could result in significant improvements in specific strength and stiffness, allowing for higher internal pressure loading. In this work, using wet winding, CNTs were distributed into resin and then introduced into a fiber matrix. Composite cylinders were produced at various winding angles. These cylinders were tested and compared to cylinders without CNT reinforcement. This research focuses on the specific strength and stiffness of CNT-reinforced cylinders.

THIS PAGE INTENTIONALLY LEFT BLANK

TABLE OF CONTENTS

I.	INTRODUCTION.....	1
A.	BACKGROUND	1
B.	LITERATURE REVIEW	3
C.	OBJECTIVES	4
II.	CONSTRUCTION OF COMPOSITE CYLINDER.....	5
A.	GENERAL.....	5
B.	CYLINDER FABRICATION.....	6
C.	CNT MIXING AND ADDITION	9
D.	CURING PROCESS.....	11
E.	MACHINING PROCESS	11
III.	EXPERIMENT	13
A.	TESTING DEVICES.....	13
B.	TESTING PLAN.....	15
C.	PROCEDURE	15
D.	RAM AND WEDGE FREE BODY DIAGRAM.....	15
E.	FRICTION COEFFICIENT.....	16
F.	BURST PRESSURE CALCULATION	17
G.	YOUNG’S MODULUS.....	17
IV.	RESULTS	19
A.	70 DEGREE CYLINDER	19
B.	75 DEGREE CYLINDER	28
C.	85 DEGREE CYLINDER	37
D.	SUMMARY OF RESULTS	46
V.	CONCLUSIONS, RECOMMENDATIONS, AND FUTURE WORK	51
A.	CONCLUSIONS AND RECOMMENDATIONS.....	51
B.	FUTURE WORK.....	52
	LIST OF REFERENCES	55
	INITIAL DISTRIBUTION LIST	57

THIS PAGE INTENTIONALLY LEFT BLANK

LIST OF FIGURES

Figure 1.	USV Conducting Sea Trials. Source: [2].	2
Figure 2.	F-35 Aircraft Conducting Operations. Source: [3].	2
Figure 3.	Composite Cylinder Produced by Ponshock. Adapted from [6].	3
Figure 4.	X-Winder 4-Axis 4X-34	5
Figure 5.	Mold Release, Receipt Paper, and Shrink Wrap	6
Figure 6.	Resin/Hardener and Mixing Materials	8
Figure 7.	Winding Angle Represented on the X-Winder Machine	9
Figure 8.	CNT Wet Bath from the X-Winder Machine	10
Figure 9.	Cylinder Post-processed and Just Prior to Testing	11
Figure 10.	Wedge and Ram Testing Device. Source: [6].	13
Figure 11.	Testing Device Staging	14
Figure 12.	Free Body Diagram for Ram. Adapted from [6].	16
Figure 13.	Free Body Diagram for Wedge. Adapted from [6].	16
Figure 14.	70 Degree Cylinder Burst Pressure	19
Figure 15.	70 Degree Cylinder Hoop Strain	20
Figure 16.	70 Degree Cylinder Modulus	21
Figure 17.	Failure Patterns Observed in 70 Degree Samples	22
Figure 18.	Load-Displacement Diagram for 70 Degree Control Samples	23
Figure 19.	Load-Displacement Diagram for 70 Degree 0.05% CNT	24
Figure 20.	Load-Displacement Diagram for 70 Degree 0.10% CNT	25
Figure 21.	70 degree 0.15% CNT Load-Displacement Diagram	26
Figure 22.	70 Degree Run Comparison	27
Figure 23.	75 Degree Cylinder Burst Pressure	29

Figure 24.	75 Degree Cylinder Hoop Strain.....	29
Figure 25.	75 Degree Cylinder Modulus.....	30
Figure 26.	Failure Patterns Observed in 75 Degree Samples.....	31
Figure 27.	75 Degree Control Load-Displacement Diagram	32
Figure 28.	75 Degree 0.05 wt % Load-Displacement Diagram	33
Figure 29.	75 degree 0.10 wt% Load-Displacement Diagram	34
Figure 30.	75 degree 0.15 wt% Load-Displacement Diagram	35
Figure 31.	75 Degree Run Comparison.....	36
Figure 32.	85 Degree Cylinder Hoop Strain.....	38
Figure 33.	85 Degree Cylinder Hoop Strain.....	38
Figure 34.	85 Degree Cylinder Modulus.....	39
Figure 35.	Failure Modes Observed in 85 Degree Samples.....	40
Figure 36.	85 Degree Control Load-Displacement Diagram	41
Figure 37.	85 Degree 0.05 wt% Load-Displacement Diagram	42
Figure 38.	85 Degree 0.10 wt% Load-Displacement Diagram	43
Figure 39.	85 Degree 0.15 wt% Load-Displacement Diagram	44
Figure 40.	85 Degree Run Comparison.....	45
Figure 41.	Control Cylinders Burst Pressure	47
Figure 42.	0.15 wt% Cylinders Burst Pressure	48
Figure 43.	Hoop Strain from All Samples.....	48
Figure 44.	Observed Cylinder Failure Patterns Diagram	49

LIST OF TABLES

Table 1.	Mixing/Cooling Rates for CNT/Resin	10
Table 2.	Experimentally Determined Friction Coefficient	17
Table 3.	Overall Results for 70 Degree Cylinder.....	28
Table 4.	Overall Results for 75 Degree Cylinder.....	37
Table 5.	Overall Results for 85 Degree Cylinder.....	46
Table 6.	Observed Failure Patterns by Test	50

THIS PAGE INTENTIONALLY LEFT BLANK

ACKNOWLEDGMENTS

I would first like to thank my supportive wife, Brijet. I am forever grateful for your active encouragement and selfless attitude. Without you, none of this would be possible.

I would like to thank my advisor, Distinguished Professor Young Kwon. Your thoughtful guidance through this adventure has made all the difference.

I have much appreciation for Commander Todd Greene for being a compassionate leader. You've aided me in more ways than one, and my family will always hold you in the highest esteem.

Professor Claudia Luhrs is another amazing mentor and always quick to provide insight when needed. Thank you so much for the meetings and advice.

Thank you to Kathy Mann and Justin Laddusaw for being the best lab battle buddies. Group 2 is second to none!

Lastly, I would like to thank LuLu, Lady, Lana, and Kona. You helped me through some trying times and I'll always be thankful for your support.

Ethos anthropos daimon

THIS PAGE INTENTIONALLY LEFT BLANK

I. INTRODUCTION

A. BACKGROUND

1. Composite Materials

A composite material is the combination of two or more different materials. Traditionally in engineering, these combined materials work to benefit each other with their original properties. Some composite materials can exhibit similar strength properties to metals, while also remaining lightweight. These combined characteristics are useful in applications such as aerodynamics, ship design, structures and other applications.

Most composites are comprised of a matrix and a reinforcement. One popular example is reinforced concrete where steel bars are used to support a concrete span. Recent research in composites has investigated the reinforcement of Carbon Fiber Reinforced Polymer using a vinyl ester resin matrix, more specifically, in application of internal pressure vessels.

2. Carbon Nanotubes

Carbon nanotubes (CNTs) are on the forefront of material science. They have demonstrated a plethora of fascinating abilities, such as, conductivity, strength, and thermal reactivity. Combining CNTs within composite materials produces a lightweight structure with enhanced strength properties [1]. This strong and lightweight application could offer the Department of Defense many solutions to problems requiring a material such as this one. The next step is to test CNT reinforcement in composite fiber (CNFP) cylinders and validate the cylinder's specific strength. Furthermore, the proper percentage of nanotubes added should be recorded.

3. Defense Applications

CNFP has already started to be used in industry. One of the most well-known cases is from Zyvex Performance Materials [2]. Zyvex recently revealed a design for an unmanned service vehicle (USV) constructed from CNFP. Another example is the use of CNFP in the F-35. The F-35 aircraft is the first mass produced aircraft that will have part

of its structure built with CNFP [3]. Figure 1 displays a USV during sea trial testing. Figure 2 is a F-35 conducting operations.



Figure 1. USV Conducting Sea Trials. Source: [2].



Figure 2. F-35 Aircraft Conducting Operations. Source: [3].

One specific benefit of CNFP is that it dramatically increases the strength and toughness of a composite material without increasing its weight. In the Navy, shipbuilders are constantly looking for ways to cut weight from the ship while not impacting its strength. This is particularly lucrative in the defense industry where retaining a high material strength is necessary.

B. LITERATURE REVIEW

Many studies have investigated the effects of CNT reinforcement on CFRP. Literatures [1], [4], and [5] investigated composite/CNT relationships under various loading conditions. In the sense of CFRP composites, it's proven that CNT introduction into the composite will increase strength and fracture toughness. However, there is very little to no research on internal pressure loading. Ponshock [6] investigated the failure loading for metallic and composite cylinders and provided data for samples under internal pressure loading. Darcy [4] investigated modeling and failures of composite cylinders underneath internal pressure loadings and documented winding angles strengths and mode failure behaviors. Figure 3 shows a composite constructed from carbon fiber composite [6].



Figure 3. Composite Cylinder Produced by Ponshock. Adapted from [6].

While great strides were made to investigate internal pressure applications by both Darcy and Kwon, research on CNT reinforcement was not included. Given that CNT's are proven to increase strength and stiffness throughout many applications, it is essential to investigate their behavior with respect to their internal pressure loading.

C. OBJECTIVES

The purpose of this research is to investigate the effect of CNT reinforcement in composite cylinders under internal pressure loading. The cylinders were produced at various winding angles and CNT amounts. The specimens were then loaded onto an internal pressure applicator and put under a ramped loading until failure occurred. The cylinders were then compared amongst each other to determine the influence of winding angle and CNT reinforcement. The goal of these experiments was to determine changes in strength and stiffness with CNT reinforced cylinders and demonstrate differences amongst the various winding angles.

II. CONSTRUCTION OF COMPOSITE CYLINDER

A. GENERAL

All cylinders were wound and produced on the X-Winder 4-Axis 4X-34 (see Figure 4). A “wet winding” method was used to produce cylinders. The dry fiber would essentially run through an epoxy mixture and then be continuously wound onto a molding. The same mold was used to produce every cylinder. The mold was made of stainless steel and was hollow. Its length was 38.1 cm with an inner diameter of 6.99 cm and outer diameter of 7.62 cm. The fiber used was Torayca T700SC Dry Fiber. The nominal width was 7.26 mm and the nominal thickness was 0.10 mm. The resin used for the experiment was Pro-set M-1002-1. The hardener used was Pro-set M-2046.



Figure 4. X-Winder 4-Axis 4X-34

B. CYLINDER FABRICATION

1. Mold Setup

Prior to winding, the mold was staged on the X-winder machine. Meguir's Maximum Mold Wax Release was liberally applied to the mold three times. A break of 2–3 minutes was taken in between each application. Once the mold release was applied, the cylinder was then wrapped with a thin layer of receipt paper. Then the mold was wrapped in a thin layer of shrink wrap. Special attention was paid to not create any major bumps in order to avoid major deformities in the cylinders. Figure 5 shows the mold, receipt paper, and shrink tape used in this experiment.



Figure 5. Mold Release, Receipt Paper, and Shrink Wrap

2. X-Winder Program and G-Code

Once the mold was prepared, the winding program was launched and a code generated. The winding rate used for every cylinder was slow. The program was designed and executed one layer at a time. The code was edited to wind an extra 360 degrees on the end of each run in order to prevent slippage and promote uniformity throughout the cylinder.

3. Resin Hardener Mixing

The resin and hardener were mixed with a 4.17:1 ratio of resin to hardener in accordance with the company specifications. The mixture required hand mixing of 5 minutes. For the CNT cylinders, the resin and hardener were not mixed until the CNTs had been properly mixed into the resin (see Chapter II, Section C). Figure 6 shows the resin, hardener, and various other materials used.



Figure 6. Resin/Hardener and Mixing Materials

4. Winding Execution

Once the epoxy was ready, the mixture was loaded into the bath tray. The fiber was then fed through the winding machine and attached to the mold. Once this was done, the winding code was executed. Each cylinder was produced with 3 layers and a nominal thickness of 3 mm. The X-Winder machine was capable of winding cylinders at different angles and for this experiment winding angle was investigated as a possible source of strength for the cylinders. Figure 7 shows the winding angle and how it works with the winding process.

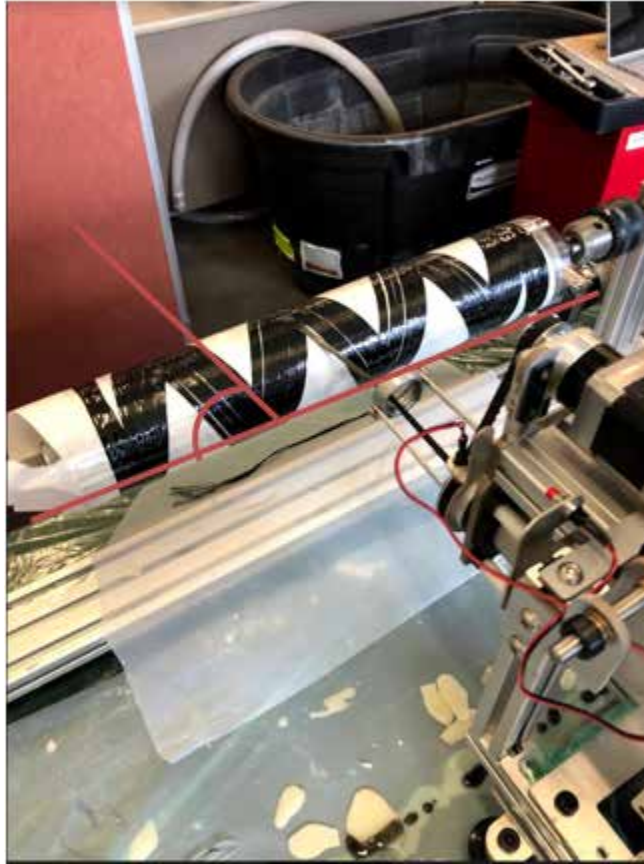


Figure 7. Winding Angle Represented on the X-Winder Machine

C. CNT MIXING AND ADDITION

1. CNT dispersion

In order to obtain the proper weight percentage, the resin was weighed and the appropriate amount of CNTs were determined based of weight percentage. The amount of CNTs required were then weighed and placed into the resin. The resin and CNTs were mixed using a FlakTek, Inc. SpeedMixer. In between each speed mixer run, the CNT/resin mixture had to be cooled to prevent overheating and degrading the CNTs. Cooling was done by submerging the mixture container in room temperature water for various times dependent on the mixing rate. Table 1 shows the mix/cooling rates and times.

Table 1. Mixing/Cooling Rates for CNT/Resin

Run 1	2000 rpm for 2 minutes
Cooling 1	3 minutes
Run 2	3000 rpm for 1 minute
Cooling 2	3 minutes
Run 3	3000 rpm for 1 minute
Cooling 3	3 minutes
Run 4	3000 rpm for 1 minute
Cooling 4	1 minute

2. CNT addition

Once the mixing was complete, the CNT/resin mix was combined with the hardener as normal. Once mixed with the hardener, the epoxy was then placed into the wet bath (see Figure 8). The program was then executed as normal. Figure 8 shows the composite fiber running through a CNT reinforced resin/hardener mixture in the X-Winder machine.

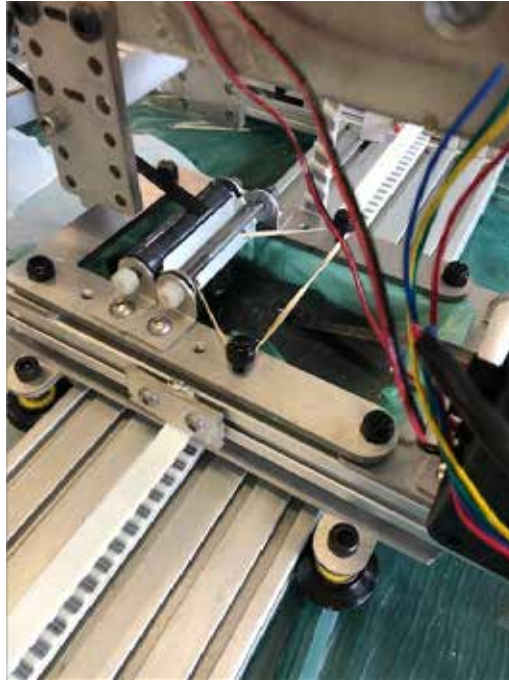


Figure 8. CNT Wet Bath from the X-Winder Machine

D. CURING PROCESS

All wet wound cylinders using the Pro-set resin/hardener mixture listed above required curing. In accordance with the specifications provided from the manufacturer, the wet wound cylinder needed to be cured for at least 6 hours at a temperature of 60 degrees Celsius. Once the cylinder was cured, it was removed from the molding and machined to 76.2 mm segments.

E. MACHINING PROCESS

The machining process required special protocols in order to prevent the fiber from splitting and tearing out. Furthermore, they had to be of accurate length and perpendicular to the axis (see Figure 9). The method used for this research was derived from literature [4]. This method proved to be the most accurate way to cut cylinders and dramatically minimized damage.



Figure 9. Cylinder Post-processed and Just Prior to Testing

THIS PAGE INTENTIONALLY LEFT BLANK

III. EXPERIMENT

A. TESTING DEVICES

1. Internal Compression Testing Device

Internal compression testing was conducted by a SATEC-operated pipe-expander. The design and analysis of the instrument was done by Ponshock [6]. The device was designed and built to ensure that there is minimal deformity while applying pressure to the interior of the cylinder.

This device was used in conjunction with a SATEC compression testing machine. This allowed an application of uniform internal pressure on the walls of the composite cylinders. The device was made of two opposing rams compressed towards each other. These rams place an outward force on eight identically machined wedges. The test cylinder was placed around these wedges. Figure 10 shows a diagram of the testing device. Figure 11 is the device staging just prior to testing.



Figure 10. Wedge and Ram Testing Device. Source: [6].



Figure 11. Testing Device Staging

2. Hoop Strain Calculation

In order to calculate strain, a formula was derived using the SATEC machine deflection. The angle of the wedge to ram was known to be 80 degrees. From this a free body diagram was drawn (see Figures 12 and 13). Then using geometry of the wedge, the hoop strain equation was derived using the deflection in the hoop direction (see Equations 1 and 2).

$$u = d \cot q \quad (1)$$

$$e_q = \frac{u}{R} \quad (2)$$

B. TESTING PLAN

This experiment was meant to investigate CNT reinforcement through various weight percentages and winding angles. Using this logic, an experiment plan was drawn. From literatures [1], [4], and [5], the appropriate weight percentage and winding angles were determined. This was based on the winding machine capability and actual experimental data. The stronger winding angles were found to be in the 70 to 80 degree angle window [4]. The appropriate weight percentage of CNTs to be added to the epoxy-resin were theorized to be in the 0.05-0.15 weight percentage [1] and [5].

C. PROCEDURE

Prior to each test, all contact surfaces subject to friction in the wedge and ram device were coated with a thin layer of Valvoline Multi-Purpose Grease for Disk Brake Wheels/Steering Linkage/Chassis/Suspension/Universal Joints. This coating helped prevent friction and damage to the device while also helping keep variation between experiments to a minimum. After lubrication, the test cylinder was loaded onto the wedges and then onto the rams. This setup was then loaded in between the pads of the SATEC machine. Once this was complete, the crosshead was lowered until it contacted the test device. From here, the load was balanced, and the gage length zeroed. Testing was complete once the specimen failed or the test device reached maximum expansion.

Maximum expansion was reached when the two rams of the testing device contacted and undertook the primary loading instead of the cylinder. Precautions were taken to adjust the SATEC limit switch to the height of the two rams. This way the machine would automatically stop in the event the two rams contacted. This was dual purpose: it protected the ram devices but also protected the machine itself from overloading.

D. RAM AND WEDGE FREE BODY DIAGRAM

Most calculations for this study required two free body diagrams of the ram and wedge device that were adapted from Ponshock's study [6]. In this study, the assumption of thin cylinder theory was used in all equations and calculations. This being based on the

fact that the nominal thickness of every cylinder was 3 mm while the nominal inner radius was 38.1 mm. Figures 12 and 13 show the free body diagrams.

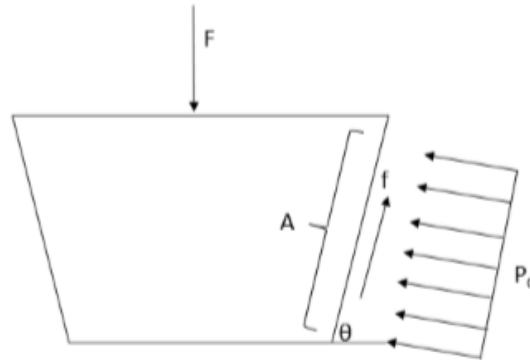


Figure 12. Free Body Diagram for Ram. Adapted from [6].

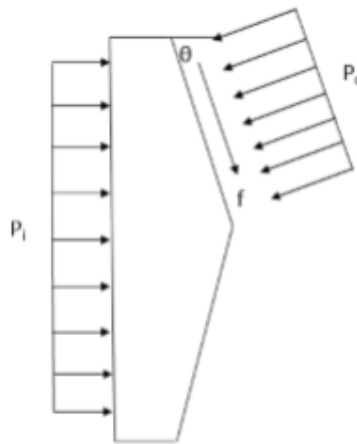


Figure 13. Free Body Diagram for Wedge. Adapted from [6].

E. FRICTION COEFFICIENT

The compression testing machine in this experiment only provided data in the form compressive force and loading. Since the machine was being repurposed for the application of pressure to cylinders, the formulas derived by Ponshock were used [6].

Prior to calculating the burst pressure, the friction coefficient of the lubricant needed to be determined. The lubricant used in the experiment was Valvoline Multi-

Purpose #2 EP Grease. In this experiment, it was necessary to determine this value on the machinery. This was conducted in the same manner as Ponshock [6]. A known material was used to determine the coefficient and thin cylinder theory was applied. In this case, an aluminum cylinder was used. Equation 3 shows the friction coefficient formulas used. Table 2 displays the results of those experiments. In this case a friction coefficient of .11 was calculated and used in all further calculations.

$$m = \frac{F \tan \phi - \mu p E L t}{\mu p E L t \tan \phi + F} \quad (3)$$

Table 2. Experimentally Determined Friction Coefficient

	Runs			
	1	2	3	Average
μ	0.15	0.09	0.1	0.11

F. BURST PRESSURE CALCULATION

In order to calculate burst pressure, formulas and derivations from [6] were used. Equation 4 shows the pressure formula used.

$$P = \frac{F}{\rho R L} \cdot \frac{\tan \phi - m}{1 + m \tan \phi} \quad (4)$$

G. YOUNG'S MODULUS

In order to calculate Young's Modulus, Equation 5 was used. This was derived from the traditional young's modulus formula and applied to a cylindrical concept. The pressure and hoop strain term are present in this formula. Because this material is anisotropic it is assumed that this modulus is an average modulus value.

$$E = \frac{P^* R}{\epsilon^* t} \quad (5)$$

THIS PAGE INTENTIONALLY LEFT BLANK

IV. RESULTS

A. 70 DEGREE CYLINDER

1. Burst Pressure

Figure 14 displays a range of data for each different type of test. The “x” denotes the mean of the data and the line within the data range denotes the median of the data set. In this case there is a strength gain associated with an increase in CNT weight percentage added. Furthermore, the 70 degree 0.10 weight percentage had only two samples available for testing. These two tests happened to display a burst pressure very close in value to each other. Also, the significant difference between the 0.15 weight percent sample and the control sample was noted. The mean value maximum value of the control sample was 12.70 MPa whereas the 0.15 weight percent sample was 27.73 MPa (see Table 3). Between the two, the strength doubled.

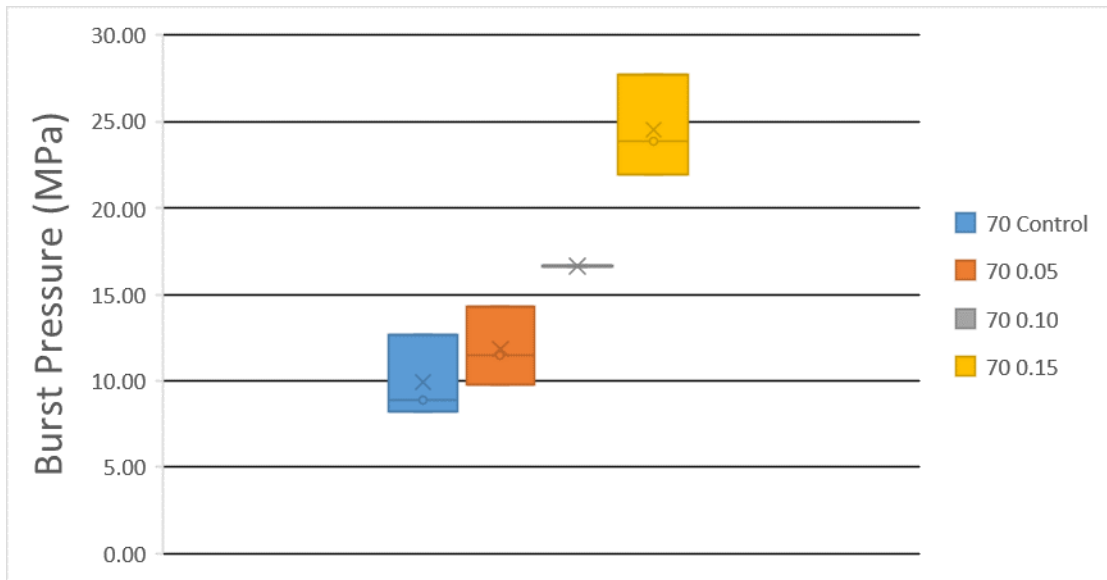


Figure 14. 70 Degree Cylinder Burst Pressure

2. Strain

The hoop strain for the 70 degree cylinders stayed within a tight grouping (see Figure 15). No observable pattern was seen as CNTs were added to the samples. Most data in this case hovered around the 0.04 m/m mark. There were no significant outliers.

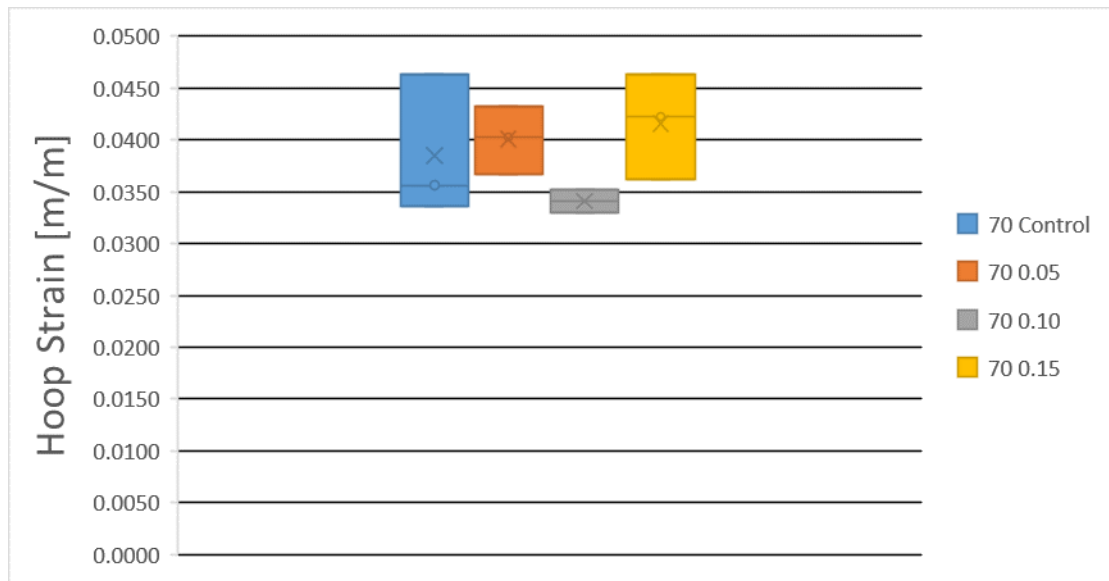


Figure 15. 70 Degree Cylinder Hoop Strain

3. Modulus

The modulus in Figure 16 correlated strongly with the increase in pressure. Since the average modulus is directly proportional to the pressure, it displays a similar trend. As the CNT amounts are increased so too is the modulus. Therefore, as CNTs were increased in the 70 degree cylinders the stiffness increased. Not only did they increased but again there was an increase of nearly double seen between the control and 0.15 weight percent samples.

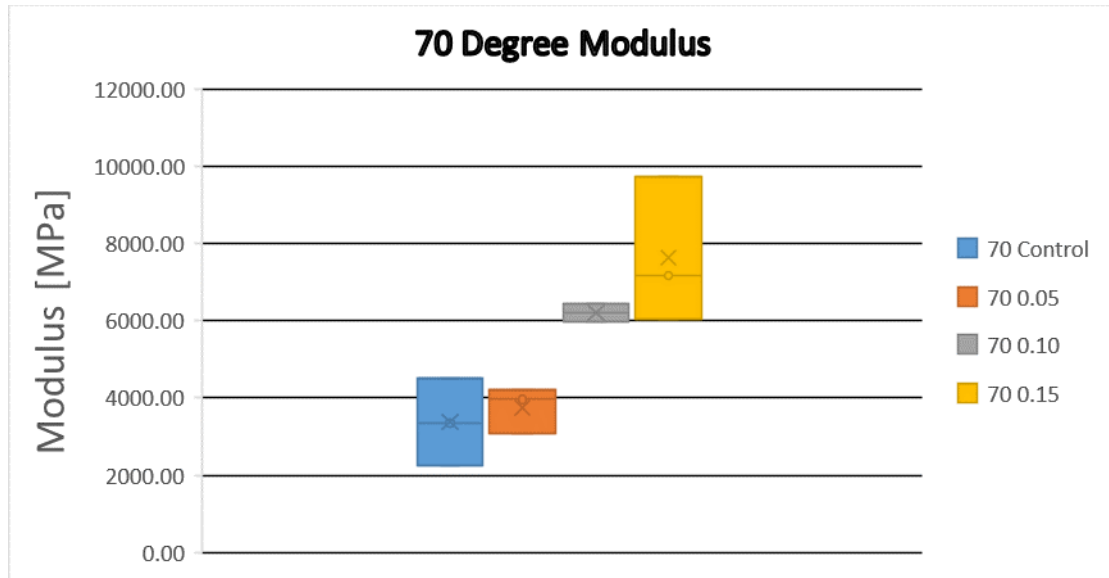


Figure 16. 70 Degree Cylinder Modulus

4. Failure Patterns

Failure patterns across 70 degree cylinders were mostly dominantly fiber failures (see Figure 17). There were four combination of fiber and matrix failures observed. One in each sample of runs. There were no discernable patterns observed as CNTs were added. Figure 44 explains the failure patterns observed. Table 6 shows the failure patterns observed across all runs and samples.



Clockwise from top left: Control, 0.05 wt % CNT, 0.15 wt % CNT, and 0.10 wt % CNT

Figure 17. Failure Patterns Observed in 70 Degree Samples

5. Load-Displacement Diagrams

In Figure 18, Run 1 and run 2 displayed similar failure loads. Run 1 and run 3 were close in slope to each other. There is also the behavior observed in run 2 where significant loading didn't occur until about 6 mm extension. This is thought to be affected by the amount of grease used in each sample. The reasoning being that the grease allow for the ram device to extend further before load is applied to the wedges.

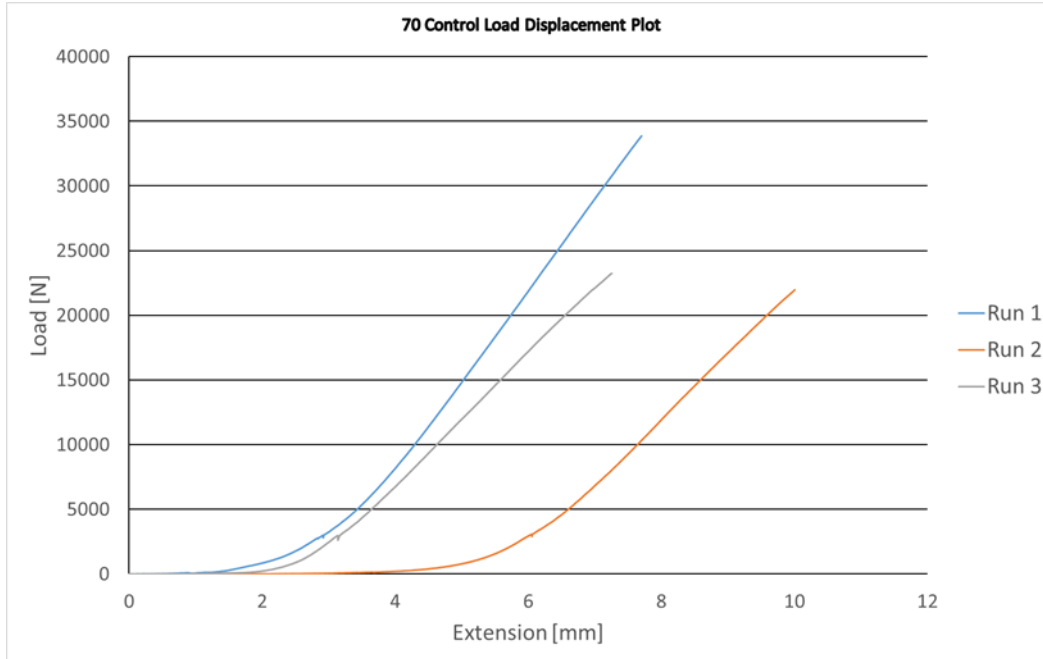


Figure 18. Load-Displacement Diagram for 70 Degree Control Samples

Figure 19 shows that all three runs having similar load-displacement curves, but their slopes do vary slightly. Run 2 and Run 3 show similar slope behavior. Ultimately, run 2 shows the highest ultimate loading.

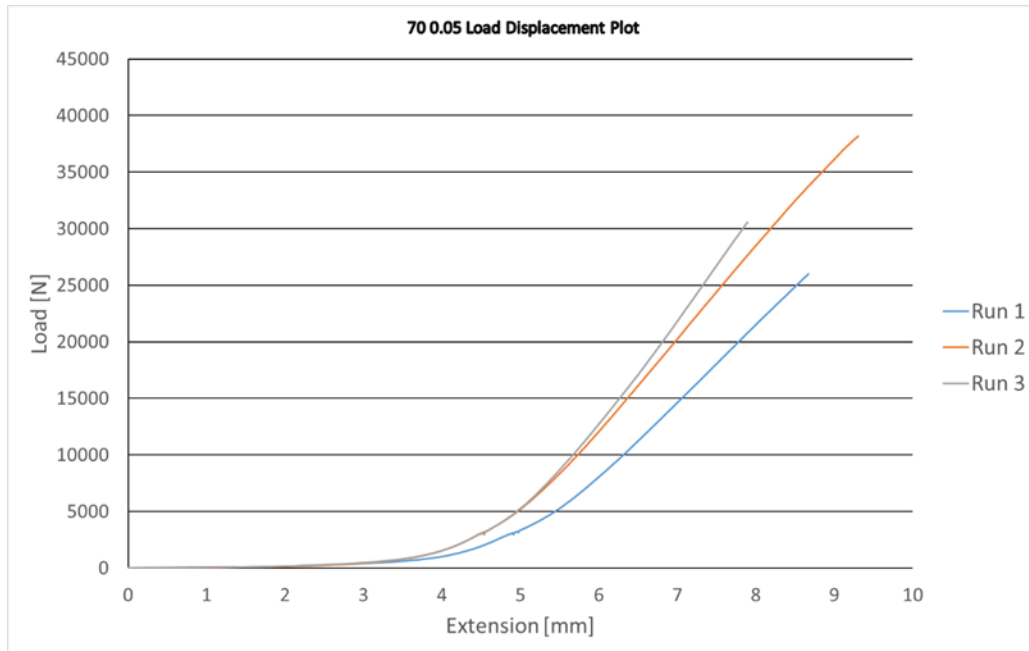


Figure 19. Load-Displacement Diagram for 70 Degree 0.05% CNT

In Figure 20, there were only 2 runs conducted. What is unique with these runs is how close their behavior is. Both show similar slope trends. Also, their ultimate load is nearly the same.

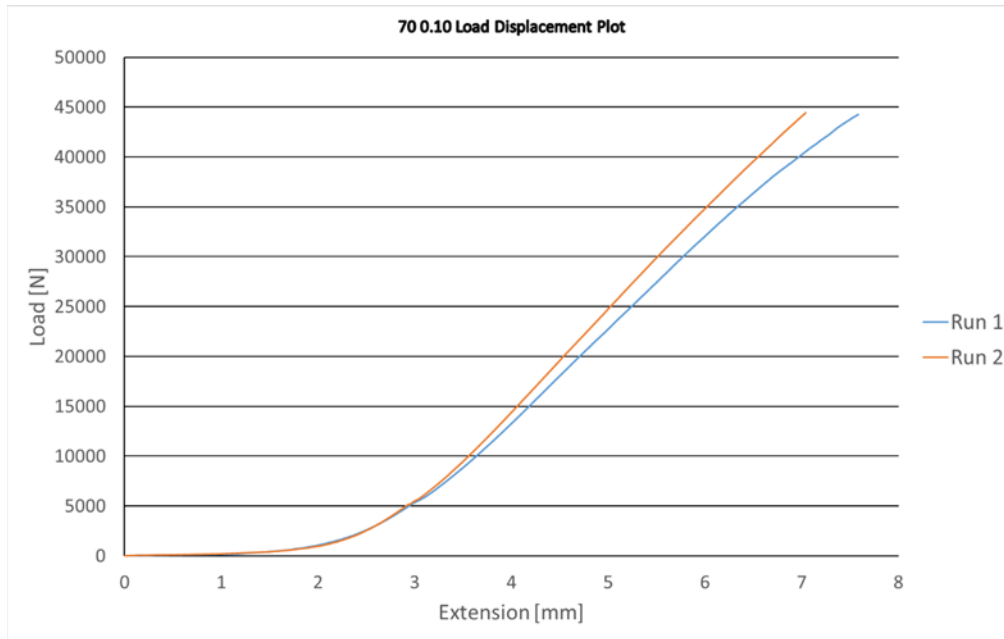


Figure 20. Load-Displacement Diagram for 70 Degree 0.10% CNT

All 3 run in Figure 21 demonstrate similar trends in terms of slope. Their extension patterns are different. Again, this is thought to be a factor of grease added to the ram/wedge device. However, all 3 exhibit comparable load-displacement tendencies.

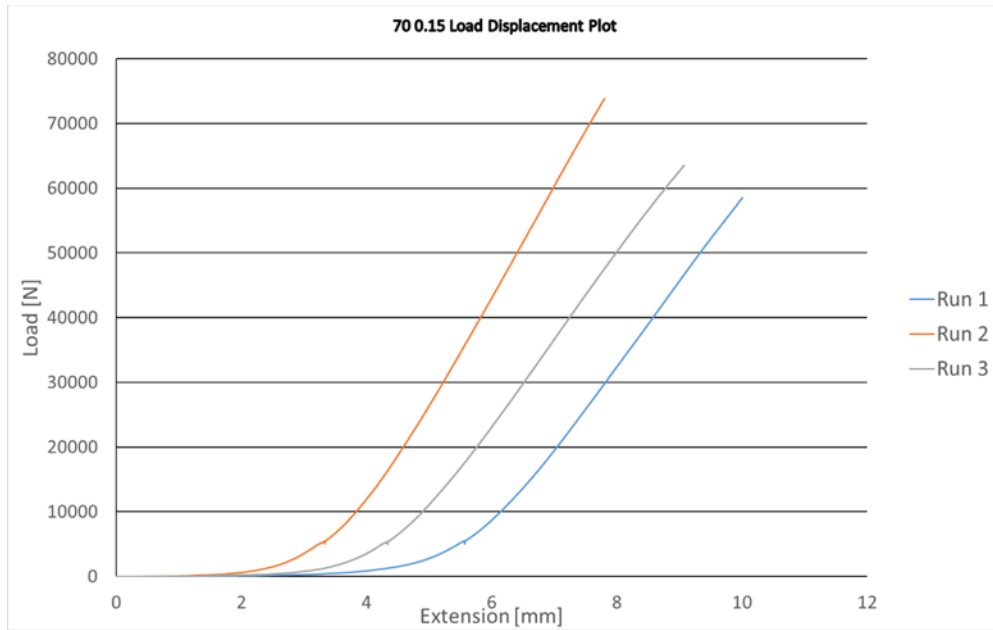
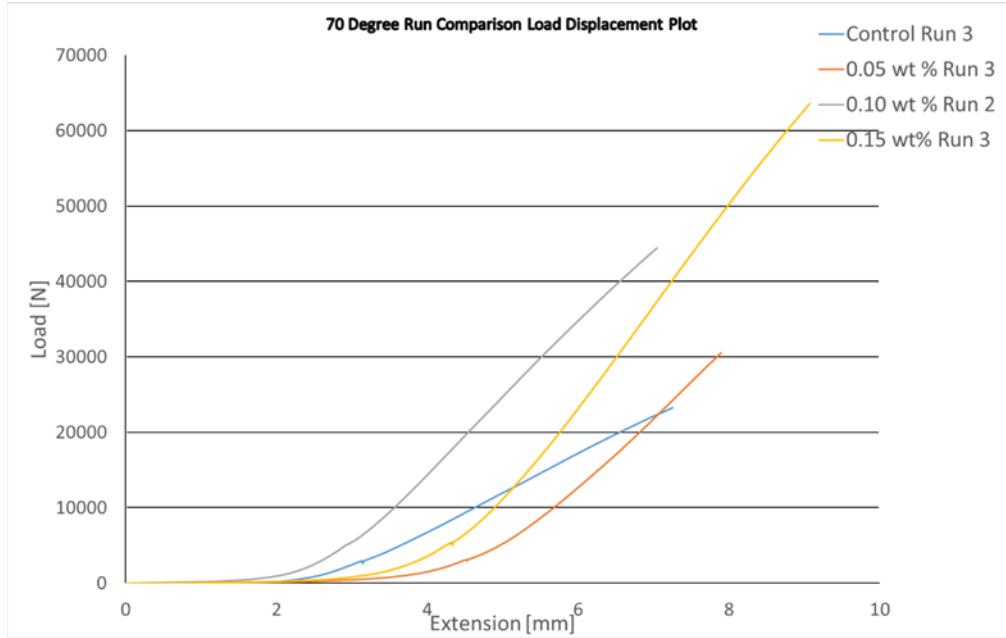


Figure 21. 70 degree 0.15% CNT Load-Displacement Diagram

In Figure 22, there is a comparison of all run 3 load-displacements with the exception of 0.10 weight percent. 0.10 weight percent only had 2 runs in this case. Therefore, run 2 was used. This plot comparison was done in order to compare the benefit of CNTs and to see the changes as more were added to the cylinder samples. A few outcomes were apparent. There is a correlation between ultimate failure and CNT weight percent. It would seem that the more CNTs added to the sample sample resulted in higher failure strength. Obviously, the positive effect would end as some point with more CNT even though the point is not known this time.



Run 2 was used for 0.10 wt% due to their being only two test samples

Figure 22. 70 Degree Run Comparison

6. Overall Results for 70 Degree Cylinder

Throughout all the winding angles, there was a parallel between ultimate loading and CNTs added. Once Equations 4 and 5 were applied, this effect was also seen with burst pressure and modulus. There was no appreciable relationship with CNTs and hoop strain in the 70 degree winging angle samples. Table 3 displays the numerical values calculated for vertical deflection (δ), hoop deflection (u), hoop strain (ϵ), burst pressure, and modulus (E).

Table 3. Overall Results for 70 Degree Cylinder

Winding Angle/CNT Amount	Run	Max δ mm	Max u mm	Max u m	Max ϵ m/m	Burst Pressure Mpa	E Mpa
70 C	1	7.698	1.357	0.0014	0.0356	12.70	4527.56
	2	10.003	1.764	0.0018	0.0463	8.24	2260.58
	3	7.255	1.279	0.0013	0.0336	8.86	3351.42
70 .05	1	8.707	1.535	0.0015	0.0403	9.76	3076.02
	2	9.343	1.647	0.0016	0.0432	14.33	4209.08
	3	7.938	1.400	0.0014	0.0367	11.47	3964.94
70 .10	1	7.613	1.342	0.0013	0.0352	16.60	5983.52
	2	7.126	1.256	0.0013	0.0330	16.69	6427.29
70 .15	1	10.001	1.764	0.0018	0.0463	21.97	6028.08
	2	7.833	1.381	0.0014	0.0363	27.73	9714.84
	3	9.122	1.608	0.0016	0.0422	23.86	7177.70

B. 75 DEGREE CYLINDER

1. Burst Pressure

Figure 23 display the same tendency seen in the 70 degree samples, in which, with an increase in CNTs there is an increase in burst pressure. The ranges seen in the 0.10 and 0.15 weight percentage runs were very wide but still displayed the strength gain trend. The control and 0.05 weight percent showed tighter grouping than the other runs.

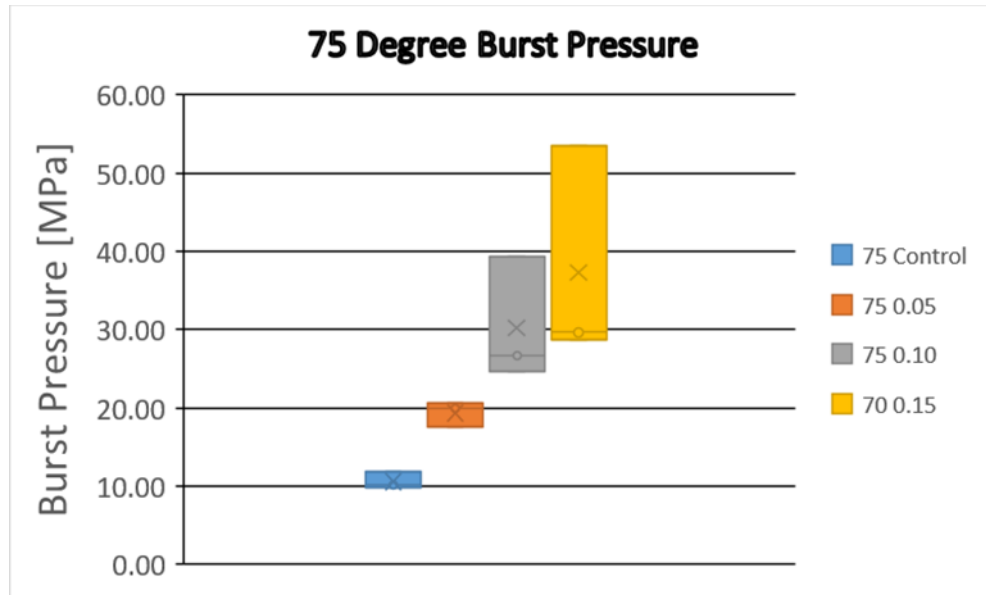


Figure 23. 75 Degree Cylinder Burst Pressure

2. Strain

The hoop strain for the 75 degree cylinders stayed within a tight grouping (see Figure 24). No observable pattern was seen as CNTs were added to the samples. Most data in this case hovered around the 0.04 m/m mark. There were no significant outliers.

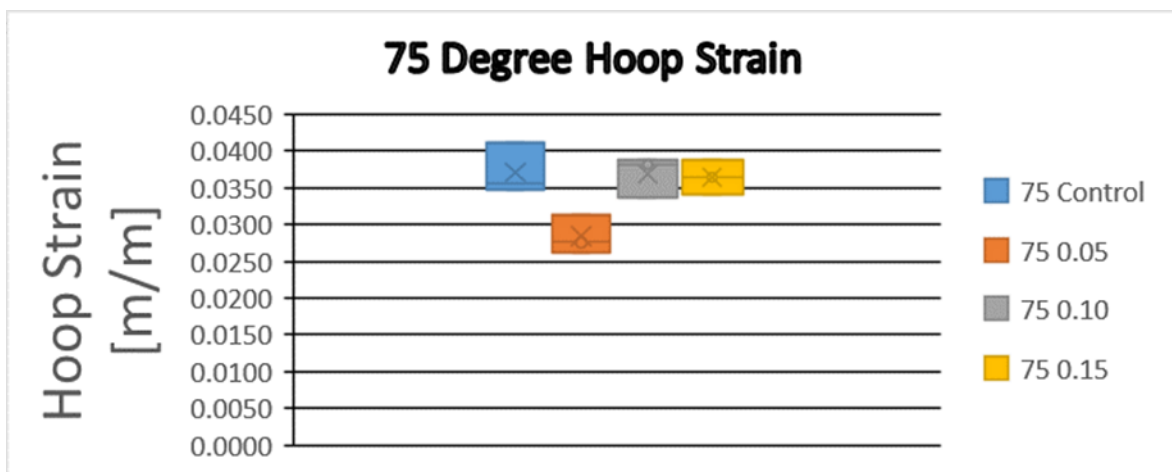


Figure 24. 75 Degree Cylinder Hoop Strain

3. Modulus

In Figure 25, there is a dramatic gain in modulus values between the CNT reinforced samples and control samples. Again the CNT and modulus gain correlation is seen here in these runs. Also, the 0.10 and 0.15 weight percentage shows a wide range while the 0.05 and control samples show a tighter grouping.

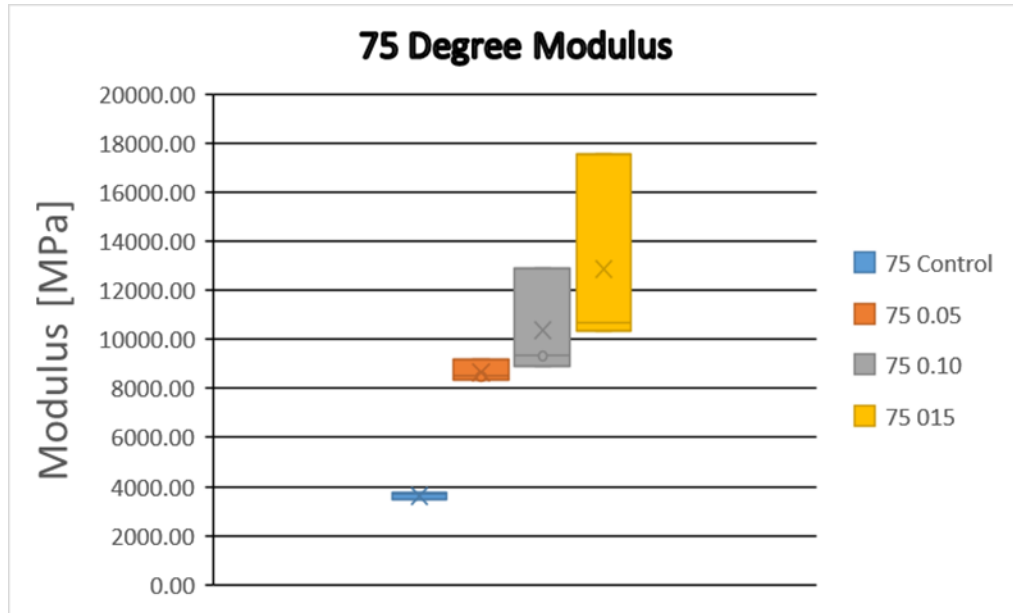


Figure 25. 75 Degree Cylinder Modulus

4. Failure Patterns

The 75 degree failure patterns differed from the 70 degree failure modes. This gives some insight into the difference between the samples. Here the most prolific failure mode was a combination between the matrix and fiber. In this case only two primary fiber failures were observed whereas, with the 70 degree samples, primary fiber failures were the majority.



Clockwise from top left: Control, 0.05 wt % CNT, 0.15 wt % CNT, and 0.10 wt % CNT

Figure 26. Failure Patterns Observed in 75 Degree Samples

5. Load-Displacement Diagrams

The slopes observed in Figure 27 were all similar. Furthermore, the ultimate failure loads were fairly close when considering the other ranges seen in samples throughout this experiment. Run 1 and run 3 were most similar in failure loading and slope.

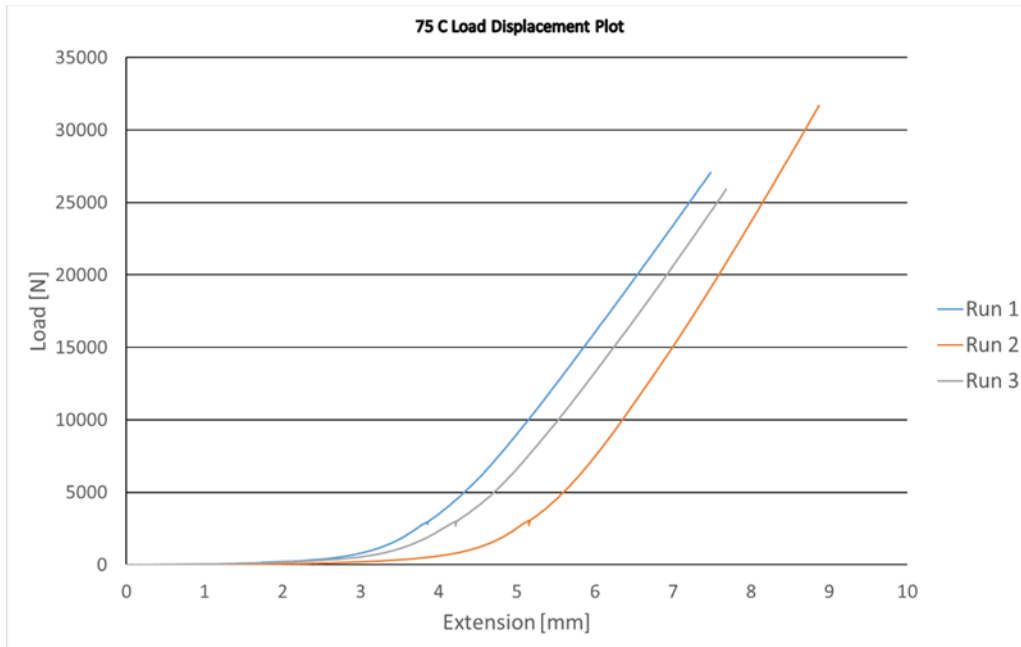


Figure 27. 75 Degree Control Load-Displacement Diagram

The 0.05 weight percentage showed runs 1 and 2 being nearly identical in slope (see Figure 28). However, their failure loading did vary slightly. Run 3 seemed to mimic the slopes of the other and closely match run 1's slope.

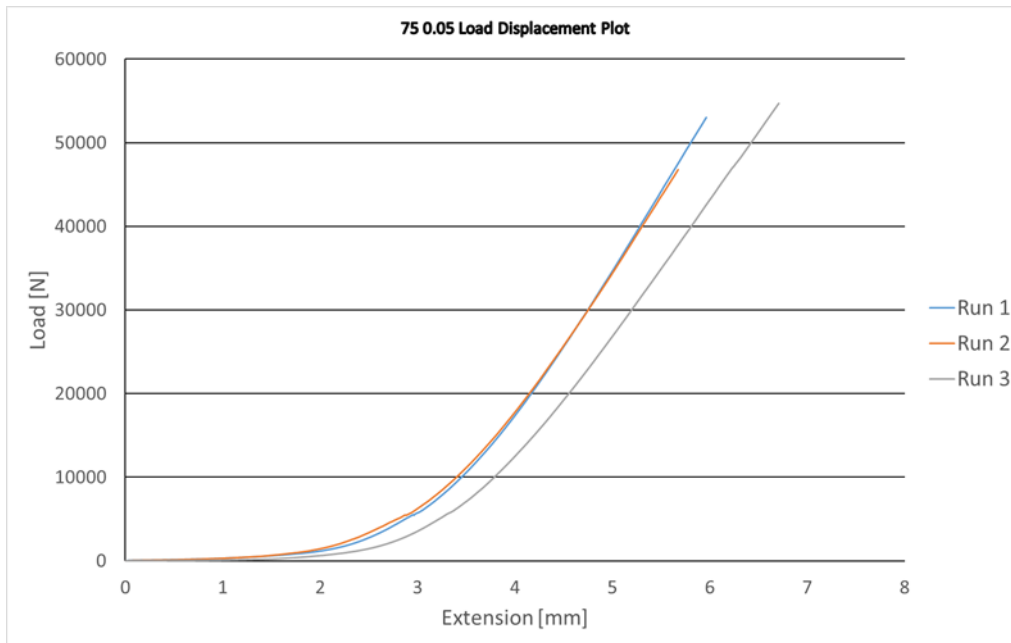


Figure 28. 75 Degree 0.05 wt % Load-Displacement Diagram

The 0.10 weight percentage had some variance throughout (see Figure 29). Run 3 noticeably varied from run 1 and 2. Run 1 and 2 were similar in slope and ultimate loading. However, run 3 had a steeper slope and failure loading that was notably higher than the others.

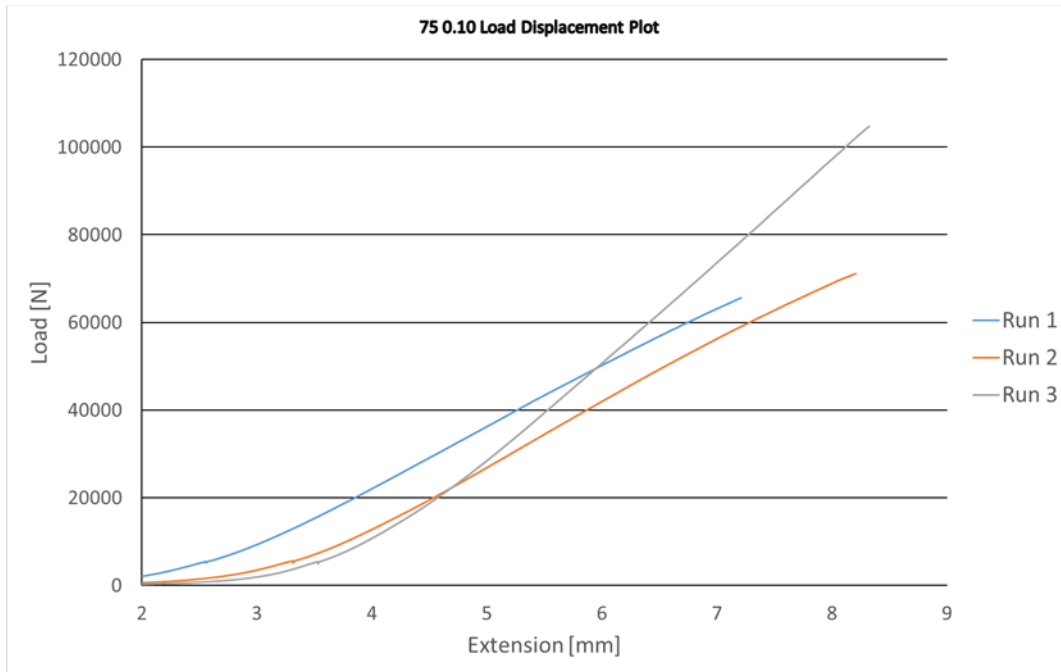


Figure 29. 75 degree 0.10 wt% Load-Displacement Diagram

In Figure 30, the loading pattern behaved in a manner similar to the 75 degree 0.10 weight percent. Run 3 had a far steeper slope than the other runs. Furthermore, the failure loading was greatly higher than run 2 and run 3. Run 2 and 3 in this case were similar in slope and loading failure. The similarity with the 0.10 sample was thought to be purely coincidence.

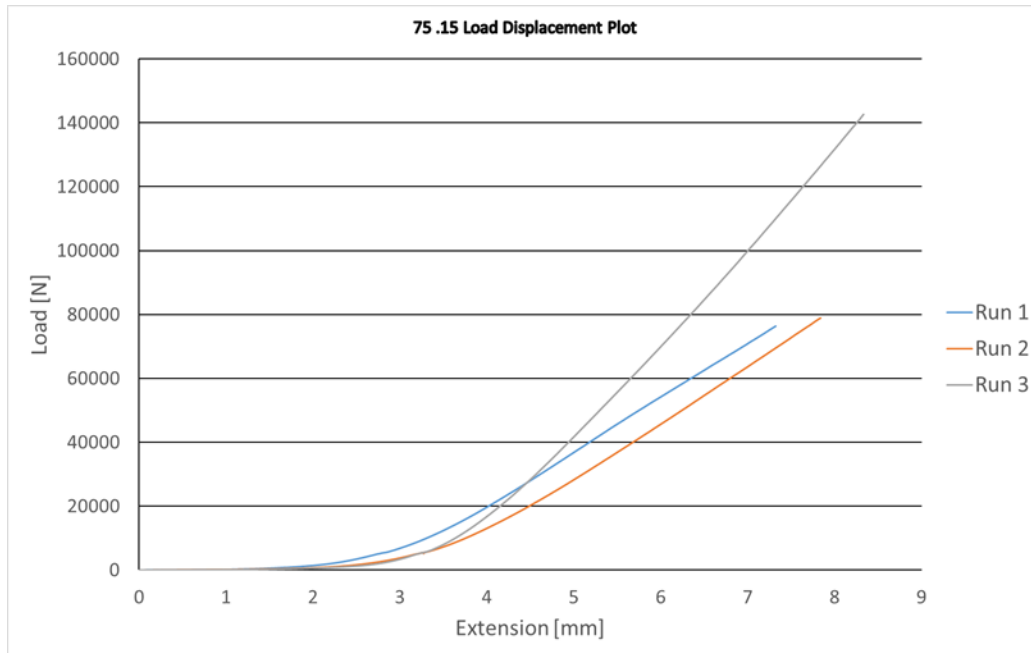


Figure 30. 75 degree 0.15 wt% Load-Displacement Diagram

The strength increase observed with CNTs and the 70 degree samples reciprocated with the 75 degree samples. In Figure 31, the run 3 of the 75 degree winding angle cylinders were compared amongst each other. Additionally, there is a perceivable pattern observed between CNT increase and the steepness of the slope. Here as CNTs increase the steepness of the slope also increases. This effect was also displayed in the 70 degree cylinders.

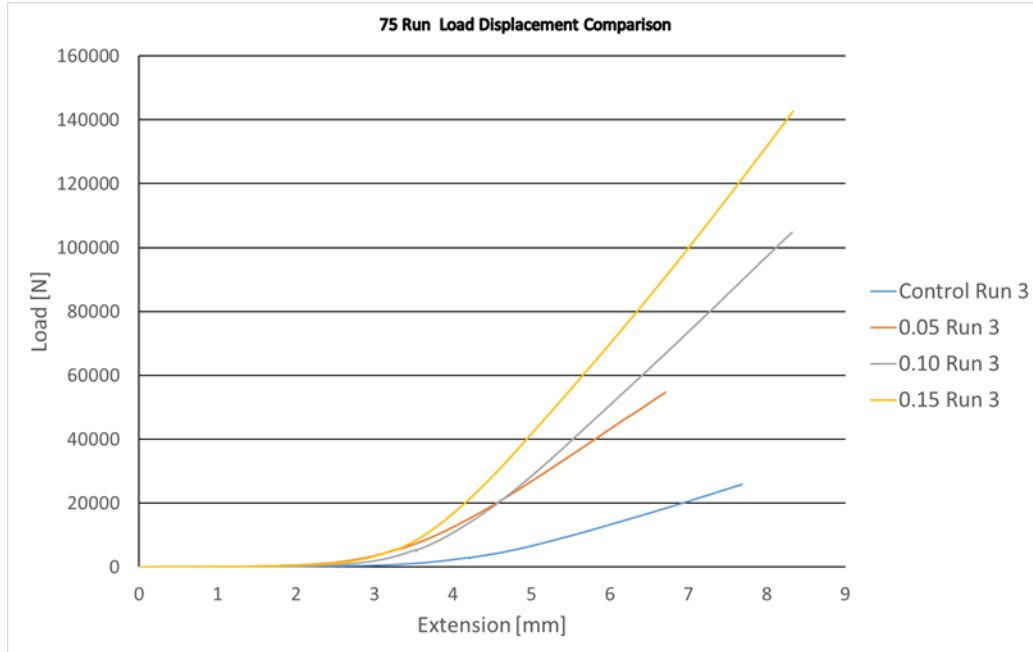


Figure 31. 75 Degree Run Comparison

6. Overall Results for 75 Degree Cylinder

Table 4 displays the numerical values calculated for vertical and horizontal displacement, hoop strain, burst pressure, and modulus. The modulus and burst pressure increased as CNT percentages went up. This corroborates the behavior seen in the load displacement graphs.

Table 4. Overall Results for 75 Degree Cylinder

Winding Angle/CNT Amount	Run	Max δ mm	Max u mm	Max u m	Max ϵ m/m	Burst Pressure Mpa	E Mpa
75 C	1	7.481	1.319	0.0013	0.0346	10.16	3726.74
	2	8.871	1.564	0.0016	0.0411	11.89	3678.12
	3	7.682	1.355	0.0014	0.0356	9.72	3472.22
75 .05	1	5.960	1.051	0.0011	0.0276	19.89	9157.57
	2	5.675	1.001	0.0010	0.0263	17.56	8491.59
	3	6.769	1.193	0.0012	0.0313	20.53	8323.45
75 .10	1	7.250	1.278	0.0013	0.0336	24.63	9322.58
	2	8.250	1.455	0.0015	0.0382	26.71	8884.44
	3	8.360	1.474	0.0015	0.0387	39.32	12906.76
75 .15	1	7.360	1.298	0.0013	0.0341	28.66	10685.83
	2	7.860	1.386	0.0014	0.0364	29.62	10341.24
	3	8.380	1.478	0.0015	0.0388	53.54	17532.52

C. 85 DEGREE CYLINDER

1. Burst Pressure

Figure 32 shows the burst pressure results from the 85 degree winding angle samples. Notice how 0.10 weight percent range falls within the range for the 0.15 weight percent. Nonetheless, the maximum value for the 0.15 weight percentage exceeds that of the 0.10 weight percent. This corroborates the strength gain trend seen in the previous samples. Here the control sample grouping had a wider range than the other angles.

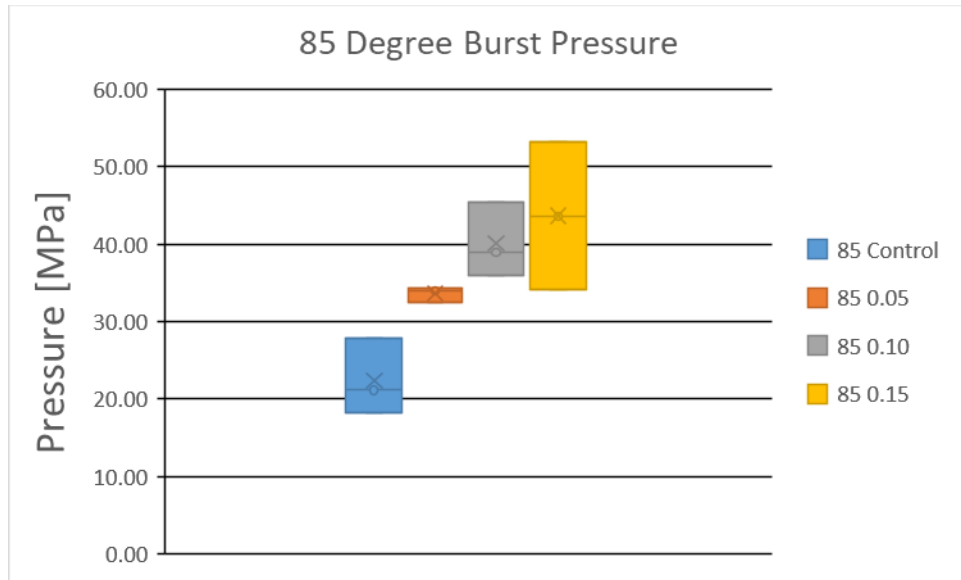


Figure 32. 85 Degree Cylinder Hoop Strain

2. Hoop Strain

The hoop strain in the 85 degree cylinders showed a lot of variance throughout but the range of values were all fairly close to each other. In Figure 33, this was the only pattern observed. There was no discernable increase in strain as CNTs were added to the samples.

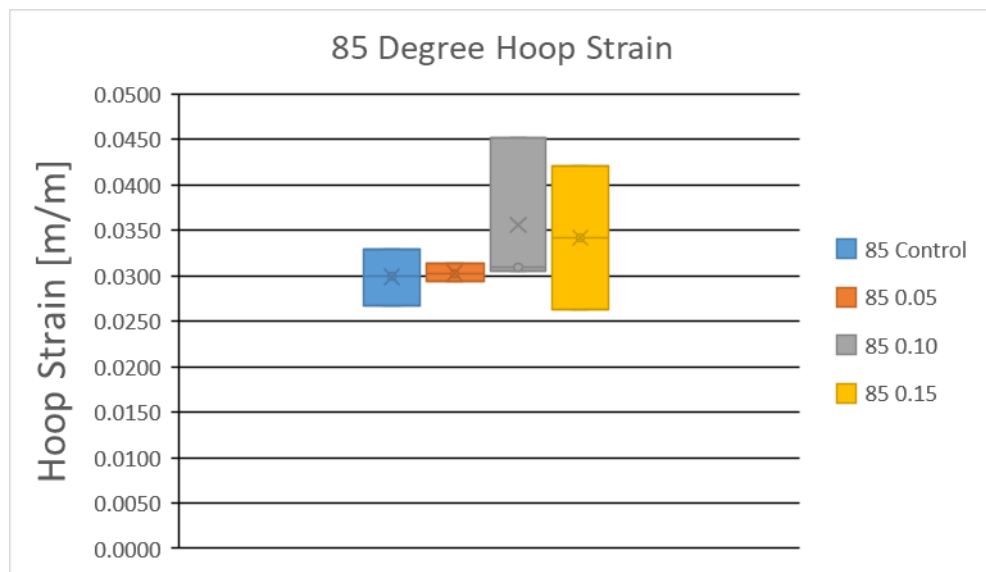


Figure 33. 85 Degree Cylinder Hoop Strain

3. Modulus

The modulus values tied in with CNT addition. Here the 0.15 weight percent samples were more closely group than the others. Furthermore, there was a stark difference between the control and CNT samples. The 0.10 weight percentage had the biggest range. Figure 34 shows this data in graph form below.

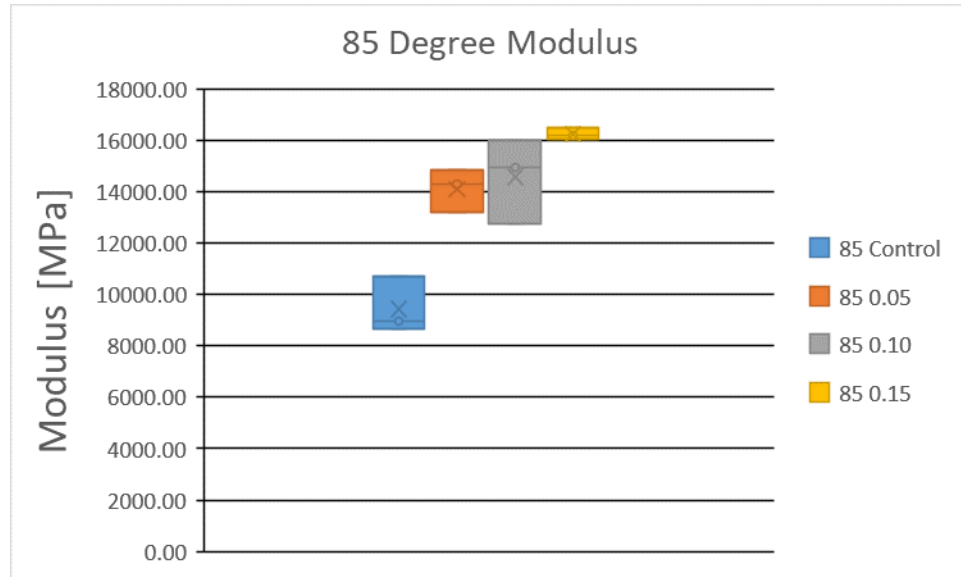


Figure 34. 85 Degree Cylinder Modulus

4. Failure Modes

In Figure 35, the control samples were all combination between fiber and matrix failures. However, with all CNT influenced samples, a dominant matrix failure was observed. These samples are the only matrix failures displayed throughout the experiment.



Clockwise from top left: Control, 0.05 wt % CNT, 0.15 wt % CNT, and 0.10 wt % CNT

Figure 35. Failure Modes Observed in 85 Degree Samples

5. Load-Displacement Diagrams

The control winding angle showed a very similar slope throughout (see Figure 35). This implies the stiffness throughout these samples are close in value. The ultimate failures had some variance.

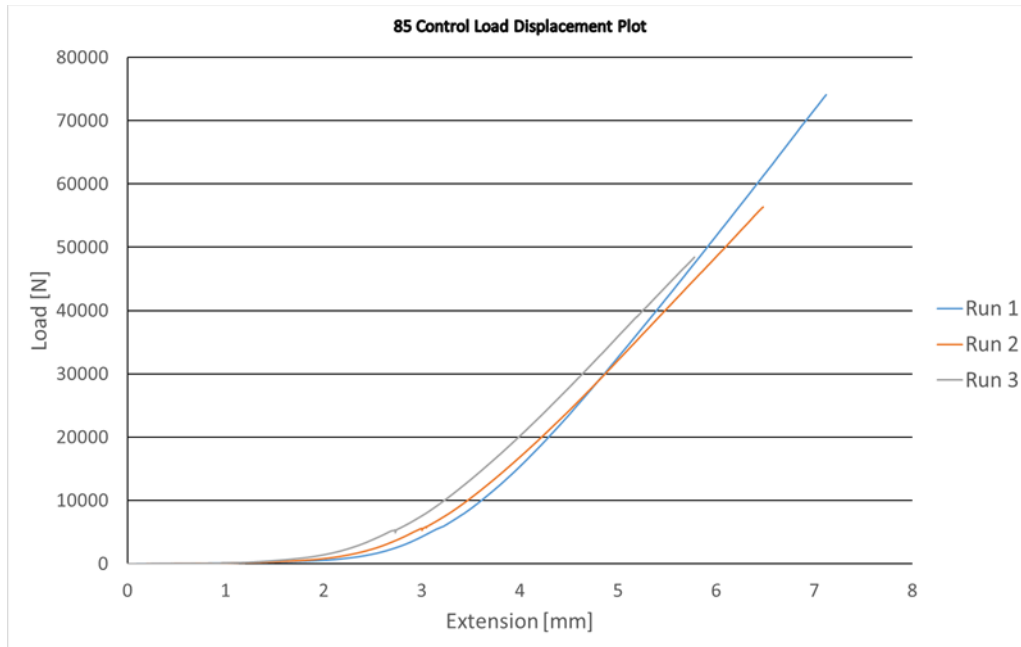


Figure 36. 85 Degree Control Load-Displacement Diagram

In Figure 37, the slopes are in common. This is corroborated by the tight grouping seen in the modulus plot (Figure 34). More interesting is that the ultimate failure loads occur within a relatively close range.

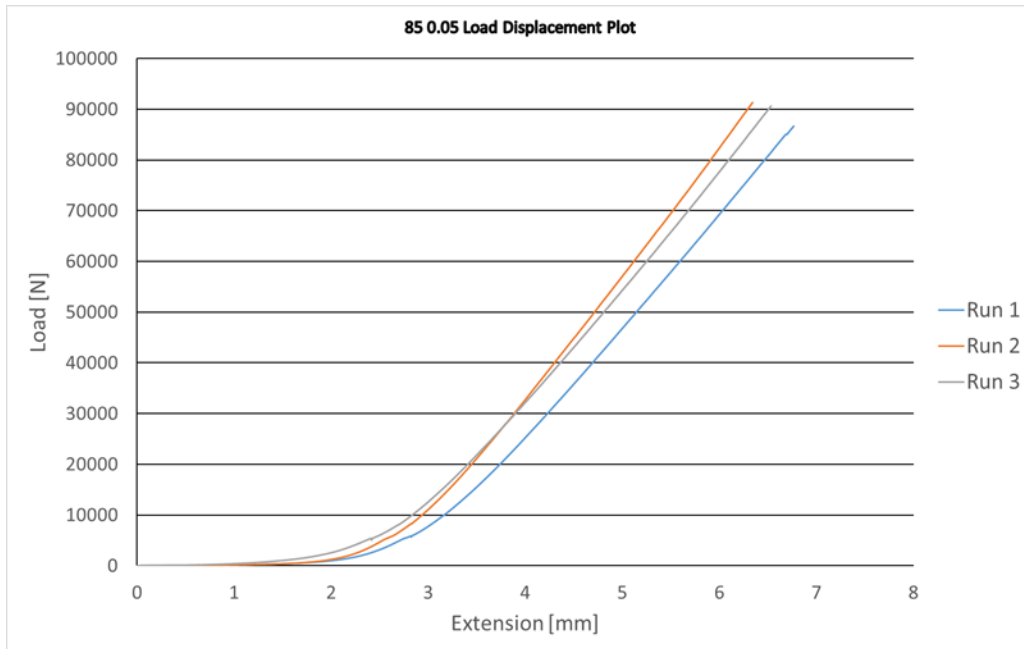


Figure 37. 85 Degree 0.05 wt% Load-Displacement Diagram

Figure 38 shows all runs share a similar slope. The run 3 had a different extension pattern. This is linked to grease application affecting ram extension. Run 3 has the largest loading. Run 1 and 2 are close in load value.

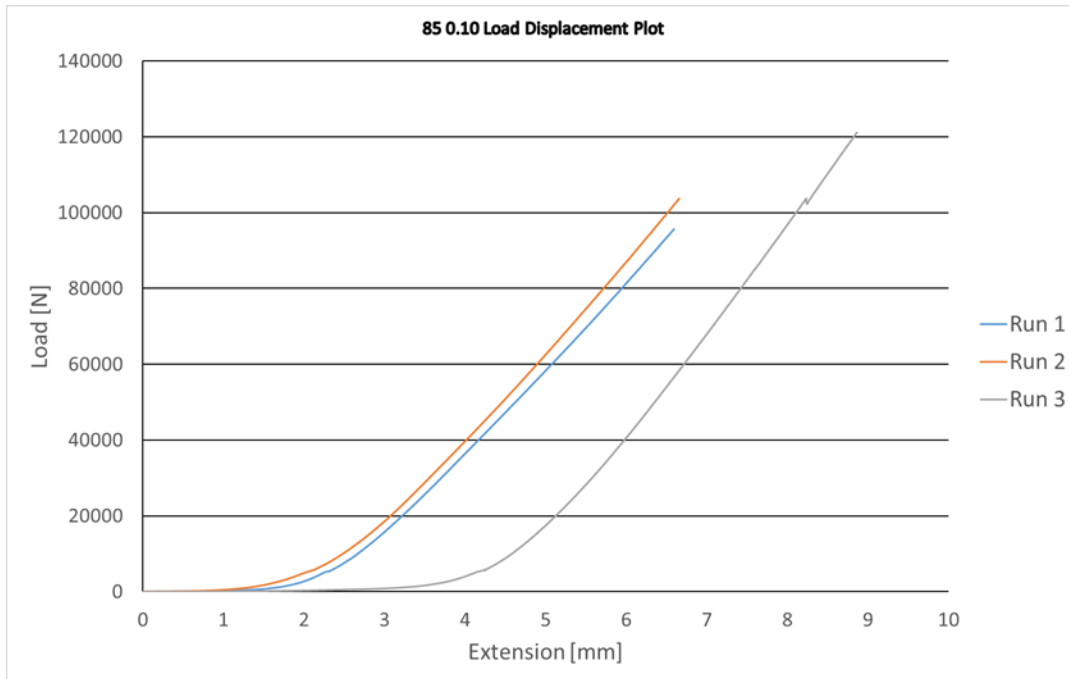


Figure 38. 85 Degree 0.10 wt% Load-Displacement Diagram

In Figure 39, the ultimate loading displayed some variance. Run 1 showed the smallest failure load while run 3 displayed the highest. Also, when related to the 0.10 weight percent in Figure 38, runs 1 and 2 are close in value to the loads seen there. There is some extension variance in this graph as well.

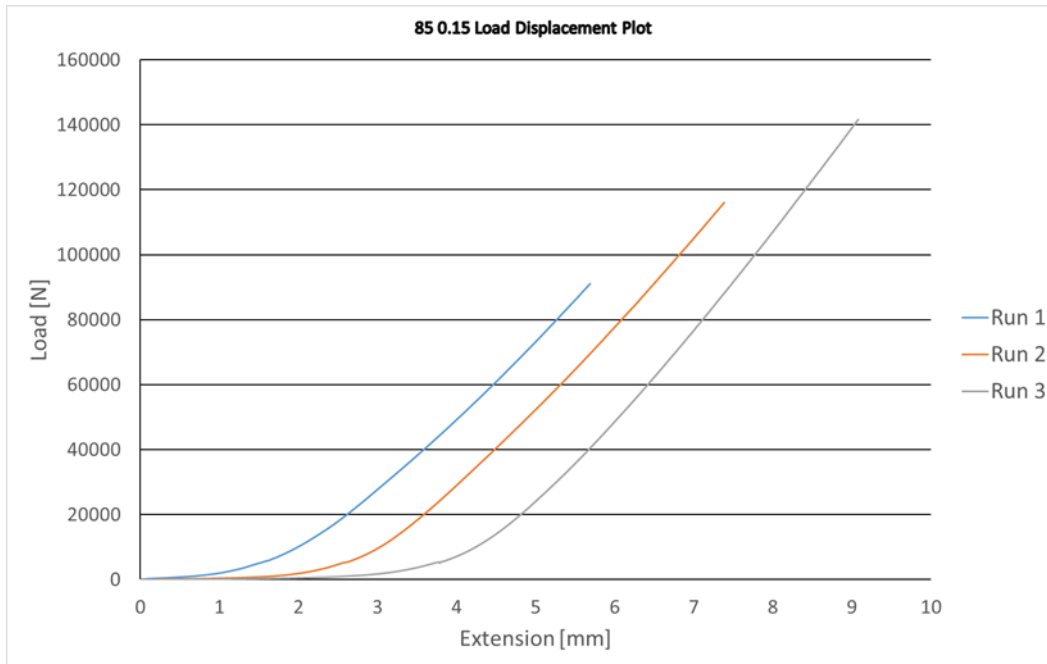


Figure 39. 85 Degree 0.15 wt% Load-Displacement Diagram

Figure 40 shows the load comparison for runs in 85 degree cylinder samples. Here the run 3 was compared. 0.10 and 0.15 both show a similar slope while 0.15 displays the highest failure loading. The control slope is less than the 0.05 weight percentage.

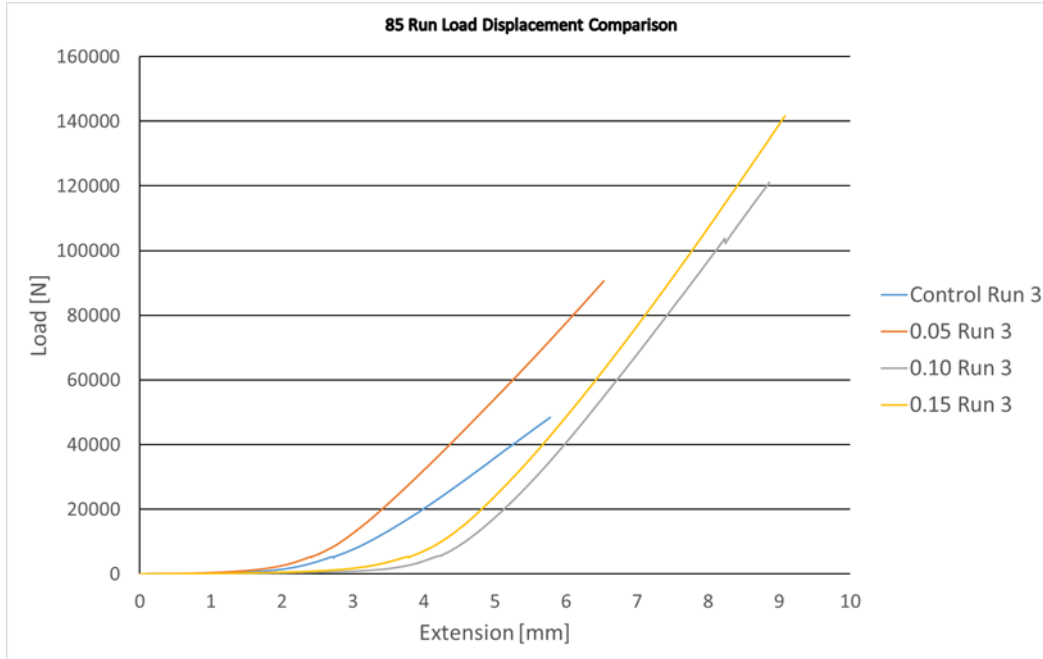


Figure 40. 85 Degree Run Comparison

6. Overall Results for 85 Degree Cylinder

Once again there is more data corroborating an increase in strength as CNTs are added to the cylinders. What is noticeably different in this case is that the 0.10 and 0.15 samples were relatively close in terms of modulus and burst pressure. This is especially the case when analyzing the other winding angles.

Table 5. Overall Results for 85 Degree Cylinder

Winding Angle/CNT Amount	Run	Max δ mm	Max u mm	Max u m	Max ϵ m/m	Burst Pressure Mpa	E Mpa
85 Control	1	7.123	1.256	0.0013	0.0330	27.81	10715.13
	2	6.476	1.142	0.0011	0.0300	21.17	8969.34
	3	5.776	1.018	0.0010	0.0267	18.18	8638.74
85 .05	1	6.766	1.193	0.0012	0.0313	32.53	13193.54
	2	6.342	1.118	0.0011	0.0293	34.28	14833.78
	3	6.532	1.152	0.0012	0.0302	34.01	14288.75
85 .10	1	6.591	1.162	0.0012	0.0305	35.90	14946.49
	2	6.683	1.178	0.0012	0.0309	38.93	15984.56
	3	9.775	1.724	0.0017	0.0452	45.46	12761.97
85 .15	1	5.688	1.003	0.0010	0.0263	34.18	16489.37
	2	7.384	1.302	0.0013	0.0342	43.56	16188.90
	3	9.078	1.601	0.0016	0.0420	53.15	16066.16

D. SUMMARY OF RESULTS

First and foremost, the analysis of specific strength and stiffness and addition CNTs were the main goals of this research. Throughout all samples there was an observed strength gain as CNTs were added. This observed correlation undoubtedly display a strong connection between CNT addition and the specific strength of composite cylinders. While there was some wide variation, an overall analysis of average strength showed a gain in strength as CNTs were added. The same benefit of the CNTs was seen with respect to the stiffness. With few exceptions, an increase in CNT concentration resulted in a corresponding increase in stiffness.

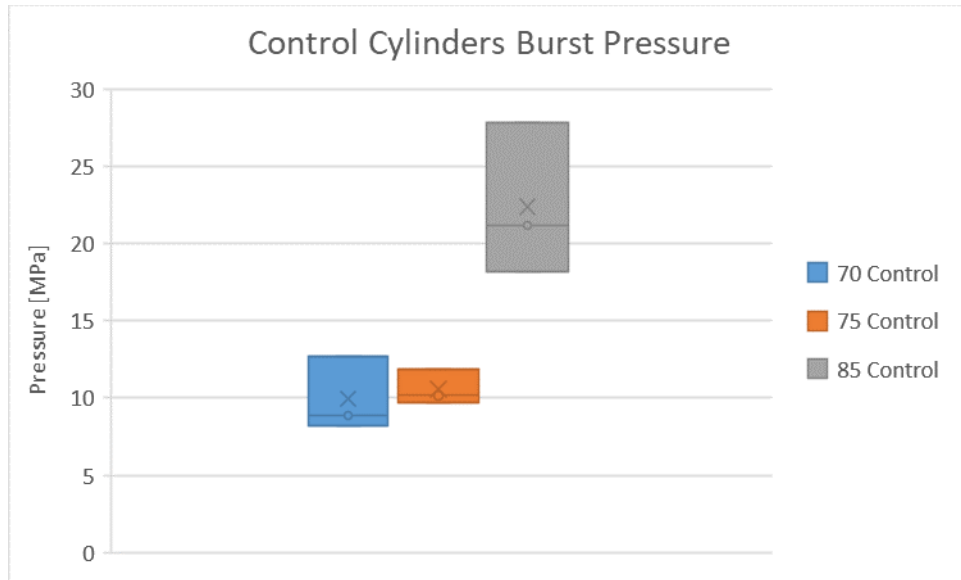


Figure 41. Control Cylinders Burst Pressure

By viewing the 0.15 weight percent samples, a strength increase was observed across winding angles (see Figure 42). While all 0.15 weight percent samples were the strongest in their winding angle pool, when compared amongst each other the 85-degree winding angle was the strongest overall. This most likely has to do with the cylinder's ability to resist hoop strain, but also axial strain due to CNT reinforcement in the epoxy resin.

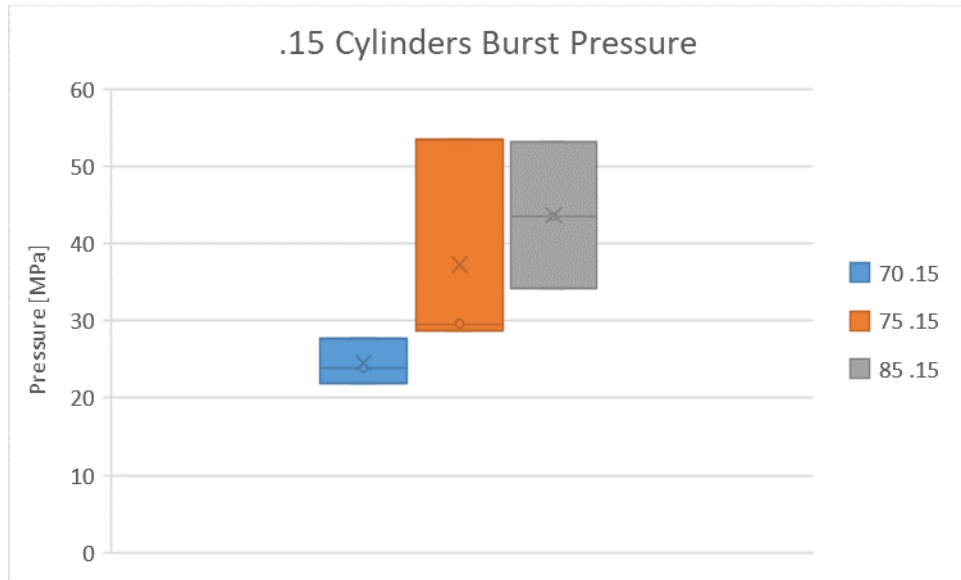


Figure 42. 0.15 wt% Cylinders Burst Pressure

Another behavior pattern observed was in hoop strain. All samples failed at similar hoop strains. There was no extreme differences amongst the data group. Figure 43 shows the hoop strain across all samples.

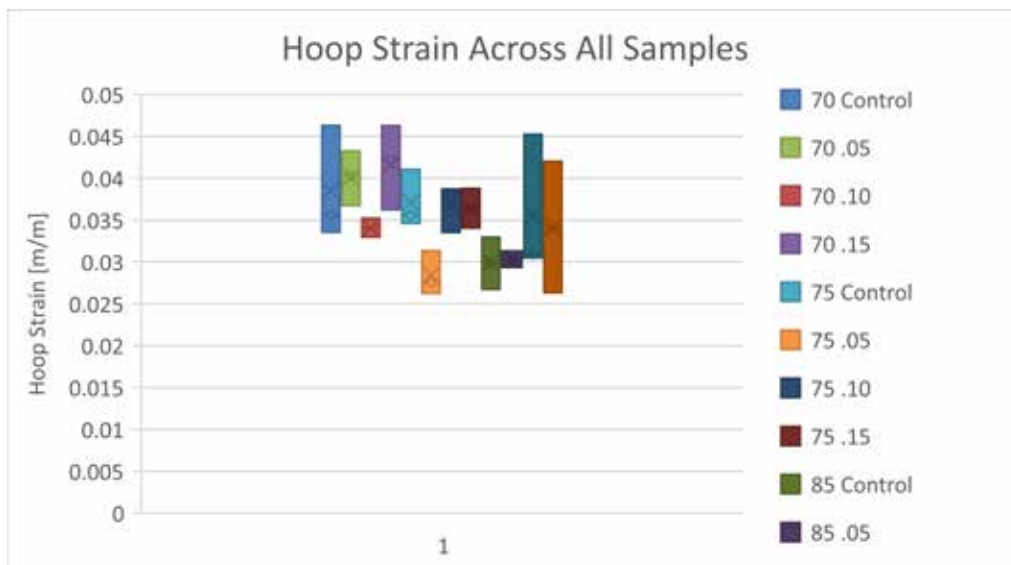
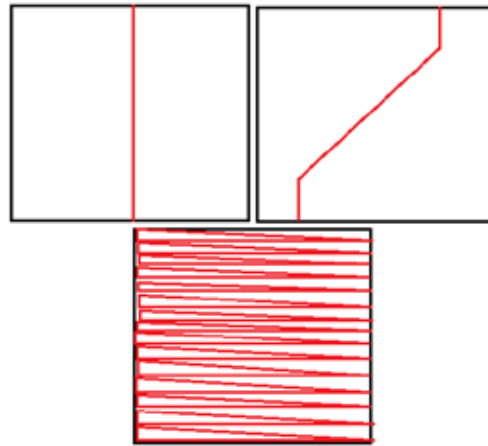


Figure 43. Hoop Strain from All Samples

The load-displacement diagram data corroborated the stiffness data and strength data. There appeared to be a distinctive change in the slope of the load-displacement diagrams as CNTs were added. A steeper slope correlated with a higher amount of CNTs. In this case, by Hooke's Law, the modulus is directly related the slope of these graphs. The average modulus found by formula 5 closely lined up with the slopes of the graph.

The failure modes in the cylinders displayed three distinct patterns of failure. These failure modes have been classified as a distinct fiber breakage, a combination of the fiber and matrix breaking, and matrix failure (see Figure 44). With this in mind, the cylinders were organized into their appropriate failure categories.



Clockwise from top left: Dominant fiber failure, combination of fiber and matrix failure, and dominant matrix failure

Figure 44. Observed Cylinder Failure Patterns Diagram

The first observable pattern to the failure patterns were trend for 70 degree cylinders to display fiber dominant failures. 75 degree cylinders showed more combination failures. The 85 degree cylinders displayed mostly matrix failures. The winding angle almost certainly adds to this trend as it can affect the stress flow within the cylinder's matrix and fiber. Table 6 shows all failure patterns observed throughout the experiment.

More interesting is the 85 degree cylinder. While its control samples were all combination of the fiber and matrix failing, its CNT samples were all matrix failures. It

appears that CNTs played a role in this trend. The other two angles did not show a distinct pattern. However, it can be said that the frequency of the combination failure became more prolific as winding angles and CNT weight percentage increased.

Table 6. Observed Failure Patterns by Test

Winding Angle	Run	Control	0.05 wt %	0.10 wt %	0.15 wt %
70	1	Dominant Fiber	Dominant Fiber	Dominant Fiber	Dominant Fiber
	2	Dominant Fiber	Combination	Dominant Fiber	Combination
	3	Combination	Dominant Fiber	Combination	Dominant Fiber
75	1	Dominant Fiber	Combination	Combination	Combination
	2	Combination	Combination	Dominant Fiber	Combination
	3	Combination	Combination	Combination	Combination
85	1	Combination	Matrix	Matrix	Matrix
	2	Combination	Matrix	Matrix	Matrix
	3	Combination	Matrix	Matrix	Matrix

V. CONCLUSIONS, RECOMMENDATIONS, AND FUTURE WORK

A. CONCLUSIONS AND RECOMMENDATIONS

There has been much research and scientific literature reporting the positive benefits of CNT reinforcement in composites. Particularly, Ref [1]. showed how CNTs can significantly increase the ultimate strength of composites. Work by Ponshock [6], helped to develop and test a machine to evaluate the failure of internal pressure vessels. This work was taken further by Darcy [4], who not only used the machine in testing but showed its applicability to gather burst strength data for internal pressure vessels. This previous work combined with this research suggests that CNT reinforcement could indeed be applicable to internal pressure vessels.

This research provided a pathway to analyze CNT reinforcement in composite cylinders in terms of internal pressure application. This study highlighted that CNT reinforcement improves strength and stiffness in this specific manner. Throughout this study, composite cylinders reinforced with CNTs displayed a higher stiffness and ultimate strength than the control samples without CNTs. Given that the CNTs showed increased strength values with very little weight gain in the samples, it can be concluded that specific strength was also increased within the CNT reinforced samples.

Furthermore, this study showed a curious trend in regard to hoop strain. All samples displayed a failure hoop strain around the same value with little variance when compared amongst the other quantitative values. This could reveal some interesting properties when it comes to CNT reinforcement and composite cylinders. Further research is clearly required, but these data imply a possible failure criterion amongst composite cylinders.

This research also analyzed winding angles produced from the X-Winder 4-Axis 4X-34 machine. The data showed a strength increase in 85-degree winding angle in the control pool. Given the small sample pool, this can't be correlated with too much certainty. However, what can be seen and observed is as winding angles increased the overall strength increased with it.

The failure modes in these cylinder tests brought forth some interesting results on CNT addition and the effect it has on the fiber and matrix of the composite cylinder. In this case a pattern existed with failure pattern, winding angle, and CNT addition. It is thought that this is directly related to the stiffness of the matrix. Darcy [4] discussed this in his model and testing. Essentially, the stiffer the matrix the more inclined you are to see a combination failure or a matrix failure.

This is most peculiar because the failure mode trend can be correlated with the modulus values increasing. The higher modulus values display matrix failures. For the most part, the median strength values displayed a combination of fiber and matrix failure. Lastly the weakest cylinders showed mostly fiber failures.

The load-displacement data slopes corroborate with the modulus and show a unique behavior in these samples. Here the correlation again corroborates that CNT addition increases stiffness and strength. There is some variance in how some samples undergo significant extension before significant loading. The cause of this is thought to be from the grease in the testing device. Since the amount of grease used wasn't controlled it's likely to have caused the device to extend less or more depending on how much was used to lubricate. However, what's important is the fact that the slopes of the load displacement graphs are similar amongst the samples. This is further corroborated by the fact that similar modulus values occurred during runs with some variation.

Finally, this study investigated the weight percentage of CNTs added to epoxy. As predicted, with an increase in weight percentage of CNTs in the epoxy mixture correlated to an observed increase in strength. This phenomenon was observed across all cylinders tested regardless of winding angle. It was most dramatic in the 85-degree cylinders and boasted strength gains nearly doubled from CNT addition.

B. FUTURE WORK

1. Loading Conditions

This experiment only worked on a standard loading condition. Further research conducted in this field should investigate various loading conditions. Loading the cylinders on an angle could be beneficial in investigating strength and failure behavior further and

advance understanding the role CNTs and winding angles play in ultimate failure. It would also be interesting to investigate the role of CNTs in exploding cylinders under blast conditions.

2. CNT Limit

This research showed a significant correlation between CNT weight percentages and strength gains. All samples tested showed an upward trend of strength gains. However, there was no limit reached on how many CNTs could be added before strength gains decreased. This should be researched further to both establish a limit in the CNT weight percentage one can add before a loss of strength is observed but also to conclude what the ultimate strength of a composite cylinder could be.

3. Hoop Strain Relationship with CNTs

Hoop strain was one behavior where the correlation between CNT weight percentage and ultimate strain was weak. This area requires a more detailed look. Given that this could be the failure criteria for these composite cylinders, it deserves more attention and investigation.

4. CNT Wettability/Fiber Bonding

There are studies that suggest the viscosity of the epoxy bonded with carbon fiber plays a significant role in the ultimate strength of the composite. This too may require a broader look. In terms of this study, the viscosity was not analyzed or noted in any way but [7] suggests the wettability and viscosity of the epoxy has an effect on the epoxy's bond with the carbon fiber. If this is true, the epoxy could be enhanced and even the samples without CNT addition could stand to have a strength gain.

5. Failure Modes

The unique failure modes amongst the cylinders requires a closer look. While in this study there was some generalization on failure patterns observed, there was no detailed investigation on failure modes and causes. This research should most definitely focus on

identifying the causes of failures amongst CNT reinforced cylinders and should attempt to look into the microscopic level; essentially a failure analysis investigation.

LIST OF REFERENCES

- [1] A. Godara et al., “Influence of carbon nanotube reinforcement on the processing and the mechanical behaviour of carbon fiber/epoxy composites,” *Carbon*, vol. 47, no. 12, pp. 2914–2923, 2009.
- [2] “Nano-fibered unmanned boat completes sea trials.” [Online]. Available: <https://www.compositesworld.com/news/nano-fibered-unmanned-boat-completes-sea-trials>. [Accessed: 08 November 2019].
- [3] “F-35 fleet surpasses 200,000 flight hours, 400th F-35 delivered.” [Online]. Available: <https://www.compositesworld.com/news/f-35-fleet-surpasses-200000-flight-hours-400th-f-35-delivered>. [Accessed: 08 November 2019].
- [4] J. Darcy, “Failure model for fibrous composites using multiscale modeling,” Ph. D. dissertation, Dept. of Mech. Eng., NPS. Monterey, CA, USA, 2019. [Online]. Available: <http://hdl.handle.net/10945/59644>
- [5] M. H. Tan, “Effects of carbon nanomaterial reinforcement on composite joints under cyclic and impact loading,” M.S. Thesis, Dept. of Mech. Eng., NPS, Monterey, CA, USA, 2012. [Online]. Available: <http://hdl.handle.net/10945/6879>
- [6] T. D. Ponshock, “Design and analysis of an experimental setup for determining the burst strength and material properties of hollow cylinders,” Defense Technical Information Center, Fort Belvoir, VA, Dec. 2015.
- [7] L. Zhang et al., “Wettability of carbon nanotube fibers,” *Carbon*, vol. 122, pp. 128–140, Oct. 2017.

THIS PAGE INTENTIONALLY LEFT BLANK

INITIAL DISTRIBUTION LIST

1. Defense Technical Information Center
Ft. Belvoir, Virginia
2. Dudley Knox Library
Naval Postgraduate School
Monterey, California